

Quantifying the effects of strength- and speed-like interventions on epidemic dynamics

Sang Woo Park^{1,*}, Kaiyuan Sun, Benjamin M. Bolker, Joshua S. Weitz, Bryan T. Grenfell, Jonathan Dushoff, [SWP: and others to be added]

¹ Department of Ecology and Evolutionary Biology, Princeton University, Princeton, NJ, USA

*Corresponding author: swp2@princeton.edu

Abstract

needed after we get comments from everyone

1 Introduction

The reproduction number \mathcal{R} —typically defined as the average number of new infections caused by an infected individual—is a key characteristic of an emerging epidemic. Its value in a fully susceptible population—the *basic* reproduction number, \mathcal{R}_0 —provides information about whether a pathogen can invade, the level of intervention required to prevent invasion, and the final size of an epidemic (Diekmann et al., 1990; Anderson and May, 1991). When an epidemic is ongoing, transmission dynamics are affected by changes in population-level immunity, non-pharmaceutical interventions, and contact patterns—these changes in transmission dynamics can be described by $\mathcal{R}(t)$, often referred to as the *effective* or *time-dependent* reproduction number (Wallinga and Teunis, 2004; Fraser, 2007; Cori et al., 2013). Interpretation and estimation of $\mathcal{R}(t)$ have been a key area of research during the ongoing COVID-19 outbreaks (Pan et al., 2020; Flaxman et al., 2020; Gostic et al., 2020).

One of the main challenges in interpreting $\mathcal{R}(t)$ can be attributed, in part, to its standard, heuristic definition: the average number of new infections caused by an infected individual. While this definition is biologically intuitive, it is mathematically imprecise as time-dependent reproduction numbers can be defined in multiple ways, depending on the cohort (e.g., a group of individuals who developed symptoms or were infected at the same time) and the types of transmission scenarios (i.e., realized or counterfactual transmission processes). Here, we primarily focus on two main measures of transmission that look at a cohort of infectees or infectors that were infected at the same time: the instantaneous reproduction number $\mathcal{R}_i(t)$ and the case reproduction number $\mathcal{R}_c(t)$.

The instantaneous reproduction number $\mathcal{R}_i(t)$ —popularized by Cori et al. (2013)—was initially defined as the “average number of people someone infected at time t

could expect to infect should conditions remain unchanged” (Fraser, 2007). While this definition is correct, we note that there are additional subtleties involved: $\mathcal{R}_i(t)$ does not depend directly on when person gets infected, only on the time point where the “conditions” are evaluated. But transmission conditions always change over the course of an epidemic due to susceptible depletion, and usually for other reasons, meaning that $\mathcal{R}_i(t)$ is a “counterfactual” quantity that does not estimate the number of people infected by any particular cohort. Nonetheless, $\mathcal{R}_i(t)$ is valuable because it provides a way of characterizing transmission conditions at time, and specifically of asking whether the disease would continue to spread if those conditions were to stay the same (Gostic et al., 2020).

The case reproduction number $\mathcal{R}_c(t)$ —popularized by Wallinga and Teunis (2004)—corresponds to the average number of new infections that an individual infected at time t generated over the course of their infection. $\mathcal{R}_c(t)$ is a realized measure, which depends on conditions after time t and can only be estimated retrospectively. Although the heuristic definition of $\mathcal{R}(t)$ (“the average number of new infections caused by an infected individual”) closely resembles that of $\mathcal{R}_c(t)$, the mathematical definitions of $\mathcal{R}(t)$ derived from standard compartmental models (e.g., basic reproduction multiplied by the proportion susceptible) actually correspond to that of $\mathcal{R}_i(t)$ (Gostic et al., 2020). Hereafter, we use $\mathcal{R}(t)$ to refer to the instantaneous reproduction number $\mathcal{R}_i(t)$ and return to the distinction between $\mathcal{R}_i(t)$ and $\mathcal{R}_c(t)$ later.

Analogous to the reproduction number \mathcal{R} , exponential growth rate r describes the speed at which infection spreads at the population level. When conditions remain the same, both \mathcal{R} and r provide equivalent threshold measures for control and are linked by the generation-interval distribution $g(\tau)$, where generation intervals describe time between infections of an infector and an infectee (Svensson, 2007). Throughout the pandemic, most analyses relied on changes in $\mathcal{R}(t)$ to evaluate the impact of intervention (Flaxman et al., 2020; Brauner et al., 2021). A few studies have adopted time-varying growth rates $r(t)$ to monitor the spread of infections, but there has been a some controversy about the relative importance of $\mathcal{R}(t)$ vs. $r(t)$. For example, Parag, Thompson, and Donnelly (Parag et al.) argued that $\mathcal{R}(t)$ is theoretically more informative than $r(t)$ when the generation-interval distribution is known and underlying assumptions about pathogen transmission hold. We have argued that they are better seen as complementary measures, with the relative value dependent on what information is available and what interventions are being considered (Dushoff and Park, 2021).

In this study, we extend the strength–speed framework of Dushoff and Park (2021) to illustrate the differences between $\mathcal{R}(t)$ and $r(t)$ in characterizing changes in epidemic dynamics. Here, epidemic “strength” and “speed” refer to the reproduction number \mathcal{R} and the growth rate r , respectively; in parallel, we use “constant-strength” and “constant-speed” interventions to refer to idealized interventions that directly affect \mathcal{R} and r , respectively. For example, a constant-strength intervention that reduces the transmission rate by a constant amount θ throughout infection can control the epidemic when $\theta > \mathcal{R}$. Analogously, a constant-speed intervention that isolates in-

80 fected individuals at a constant rate ϕ throughout infection can control the epidemic
 81 when $\phi > r$. We note that these idealized interventions are assumed to be constant
 82 across time of infection, but not necessarily across calendar time—we can imagine
 83 constant-strength and -speed interventions whose effectiveness can vary throughout
 84 an epidemic.

85 We begin by showing that the renewal process of infection can be expressed in two
 86 equivalent ways using instantaneous and case-based perspectives. The first renewal
 87 equation relies on the instantaneous reproduction number $\mathcal{R}_i(t)$, and therefore con-
 88 nects past and current incidence using a counterfactual distribution, which we call the
 89 instantaneous generation-interval distribution. The second renewal equation relies on
 90 the case reproduction number $\mathcal{R}_c(t)$, a realized measure of transmission, and there-
 91 fore connects past and current incidence using a realized distribution, which we call
 92 the forward generation-interval distribution. Instantaneous and forward generation-
 93 interval distributions differ qualitatively in the way they change through time. For
 94 example, a constant-strength intervention causes the forward distribution to change
 95 over time even though the instantaneous distribution remains invariant. On the
 96 other hand, a constant-speed intervention causes both distributions to change, which
 97 must be taken into account to correctly estimate $\mathcal{R}_i(t)$ and $\mathcal{R}_c(t)$. Instead, the time-
 98 varying growth rate $r(t)$ is a robust measure for changes in incidence under both
 99 constant-strength and constant-speed interventions as it does not require assump-
 100 tions about the underlying distribution. Finally, we use a simple SIR model as an
 101 example to demonstrate that changes in the transmission rate are equivalent to a
 102 constant-strength intervention, whereas changes in the recovery rate are equivalent
 103 to a constant-speed intervention; we note that the renewal equation theory can be
 104 generalized to more complex class of models (Champredon et al., 2018). We con-
 105 clude that $\mathcal{R}(t)$ is generally a better measure for characterizing disease spread under
 106 constant-strength interventions, whereas $r(t)$ is generally better under constant-speed
 107 interventions.

108 2 Mathematical theory

109 2.1 Renewal equation framework

110 The renewal-equation framework provides a flexible way of modeling the spread of
 111 infection and the impact of intervention (Fraser, 2007). Let $K(t, \tau)$ represent the
 112 infection kernel, defined as the rate at which secondary cases are generated at time
 113 t by an individual infected τ time units ago (we will use s, t to denote calendar time
 114 and σ, τ to denote time since infection). The shape of this kernel can depend on
 115 characteristics of the infection (e.g., variation in infectiousness over the course of
 116 infection) as well as other population-level factors (e.g., susceptible depletion, non-
 117 pharmaceutical interventions, and changes in behavior). Then, incidence of infection
 118 at time t caused by a cohort of individuals infected τ time units ago can be written

119 as the product of the kernel, $K(t, \tau)$, and incidence at time $t - \tau$, $i(t - \tau)$:

$$i_{t-\tau}(t) = K(t, \tau)i(t - \tau). \quad (1)$$

Integrating across time since infection τ allows us to express the dynamics of incidence $i(t)$ using a renewal-equation framework:

$$i(t) = \int_0^\infty K(t, \sigma)i(t - \sigma) d\sigma. \quad (2)$$

120 This formulation generalizes the dynamics of many compartmental models, including
 121 the standard SIR and SEIR models (Heesterbeek and Dietz, 1996; Diekmann and
 122 Heesterbeek, 2000; Roberts, 2004; Aldis and Roberts, 2005; Roberts and Heesterbeek,
 123 2007; Champredon et al., 2018). Throughout this paper, we focus on changes in
 124 infection and ignore complexities associated with observing infections, such as delays
 125 between infection and case reports.

Here, we show that the dynamics of this infection model can be expressed equiv-
 alently in terms of instantaneous quantities or in terms of realized quantities, mean-
 ing $\mathcal{R}_i(t)$ and $\mathcal{R}_c(t)$ with their corresponding generation-interval distributions. The
 integral of $K(t, \tau)$ across τ with t fixed gives the instantaneous reproduction num-
 ber (Fraser, 2007): $\mathcal{R}_i(t) = \int K(t, \sigma) d\sigma$. If we normalize this kernel, we get the
 instantaneous generation-interval distribution $g_t(\tau) = K(t, \tau)/\mathcal{R}_i(t)$. The instanta-
 neous reproduction number and generation-interval distribution describe (counterfactual)
 quantities that would be realized only if conditions remained constant (i.e., if
 $K(s, \tau) = K(t, \tau)$ for all $s \geq t$). The renewal equation (Eq. 2) can be rewritten using
 this decomposition:

$$i(t) = \mathcal{R}_i(t) \int_0^\infty g_t(\sigma)i(t - \sigma) d\sigma. \quad (3)$$

126 For example, if disease parameters remain constant in a simple model, such as the
 127 SEIR model, we would expect $\mathcal{R}_i(t) = \mathcal{R}_0 S(t)$ and $g_t(\tau) = g_0(\tau)$, where $g_0(\tau)$ repre-
 128 sents the intrinsic generation-interval distribution (Champredon and Dushoff, 2015).

129 Now, consider the forward kernel $F_t(\tau)$, which represents the rate at which an
 130 individual infected at time t generates secondary infections τ time units after infection:

$$F_t(\tau) = K(t + \tau, \tau). \quad (4)$$

The integral of $F_t(\tau)$, representing the total infectiousness of an individual infected
 at time t , corresponds to the case reproduction number: $\mathcal{R}_c(t) = \int F_t(\sigma) d\sigma$. The
 forward kernel, normalized by the total infectiousness, corresponds to the forward
 generation-interval distribution $f_t(\tau) = F_t(\tau)/\mathcal{R}_c(t)$, describing realized generation
 intervals for a cohort of infectors that were infected at time t . Then, the forward
 renewal equation can be written as:

$$i(t) = \int_0^\infty \mathcal{R}_c(t - \sigma)f_{t-\sigma}(\sigma)i(t - \sigma) d\sigma. \quad (5)$$

131 This forward renewal equation provides an equivalent description of the infection
 132 processes as the instantaneous form (Eq. 3).

133 We can check that the instantaneous quantities ($\mathcal{R}_i(t)$ and $g_t(\tau)$) match the
 134 forward realized quantities ($\mathcal{R}_c(t)$ and $f_t(\tau)$) when conditions remain constant (or
 135 effectively constant, as in the case of early exponential spread). Assuming that
 136 $K_s(\tau) = K_t(\tau)$ for all $s \geq t$, we obtain $F_t(\tau) = K(t, \tau)$ (and therefore, $\mathcal{R}_c(t) = \mathcal{R}_i(t)$
 137 and $f_t(\tau) = g_t(\tau)$).

138 2.2 Constant-strength and constant-speed interventions

139 To model changes in epidemic dynamics, we introduce an intervention function $\mathcal{I}(t, \tau)$
 140 which can depend on both calendar time t as well as time since infection τ . Then,
 141 the infection kernel under \mathcal{I} at calendar time t can be written as:

$$K(t, \tau) = \mathcal{R}_0 \mathcal{I}(t, \tau) g_0(\tau), \quad (6)$$

142 where g_0 is the pre-intervention instantaneous generation interval (assumed to remain
 143 nearly constant for the time period of interest, apart from the effects of the interven-
 144 tion) The forward kernel of an individual infected at time t under \mathcal{I} can then be
 145 written as:

$$F_t(\tau) = \mathcal{R}_0 \mathcal{I}(t + \tau, \tau) g_0(\tau). \quad (7)$$

146 The intervention function $\mathcal{I}(t, \tau)$ can capture any kinds of epidemiological changes,
 147 including changes in the susceptible pools $S(t)$ (either due to natural infection or
 148 vaccination) as well as introduction and lifting of non-pharmaceutical interventions.

149 We focus on two idealized interventions, which we refer to as constant-strength
 150 and constant-speed interventions, and later generalize them (Dushoff and Park, 2021).
 151 While our primary focus is on the instantaneous quantities ($\mathcal{R}_i(t)$ and $g_t(\tau)$), we
 152 first illustrate the impact of constant-strength and constant-speed interventions using
 153 forward quantities as they describe realized transmission processes and are easier to
 154 interpret. In particular, the forward kernel allows us to describe how intervention
 155 measures will affect onward transmissison of an infected individual. We present the
 156 impact of these idealized interventions on instantaneous kernels in Supplementary
 157 Materials. as we explain later, the impact of intervention measures on instantaneous
 158 kernel can be counterintuitive.

159 First, we consider a constant-strength intervention $\mathcal{I}(t, \tau) = \mathcal{P}(t)$, which reduces
 160 the transmission rate by a constant amount across the age of infection τ at a given
 161 time t ; note that $\mathcal{P}(t)$ need not be constant across calendar time. In particular, the
 162 forward kernel corresponds to $F_t(\tau) = \mathcal{R}_0 \mathcal{P}(t + \tau) g_0(\tau)$, and therefore changes in
 163 intervention \mathcal{P} across calendar time will affect the shape of the forward kernel. For
 164 example, a constant-strength intervention that reduces transmission by a factor of θ

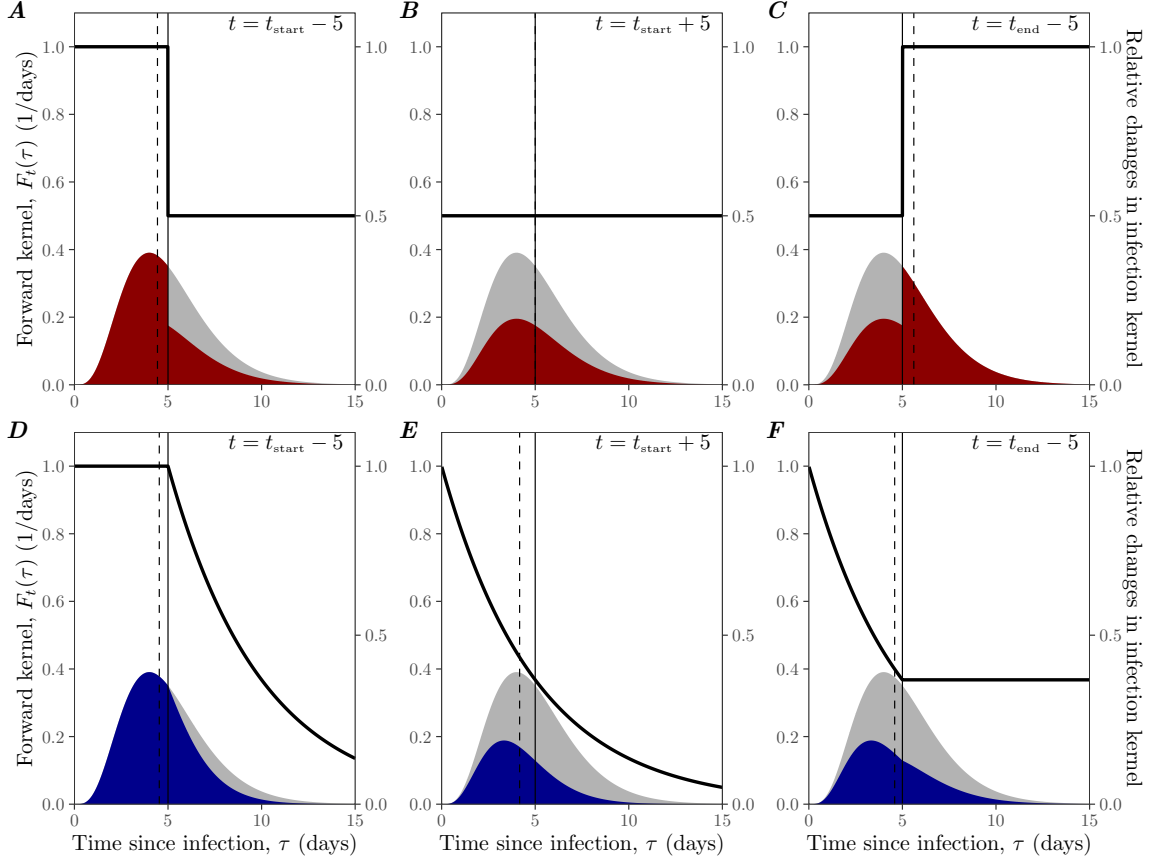


Figure 1: The impact of constant-strength and constant-speed interventions on forward kernels. The impact of constant-strength (A–C) and constant-speed (D–F) intervention on forward kernels of cohort of individuals infected at different time: 5 days before intervention onset (A, D), during intervention (B, E), and 5 days before intervention offset (C, F). Gray shaded curves represent the (fixed) intrinsic kernel $K_0(\tau)$, which is modeled using a gamma distribution with \mathcal{R}_0 of 2, a mean of 5 days and a squared coefficient of variation of 0.2. Colored curves represent the forward kernel $F_t(\tau)$ under constant-strength (A–C) and constant-strength (D–F) interventions. The constant-strength intervention is assumed to reduce kernel by a factor of 2. The constant-speed intervention is assumed to have a constant hazard of 1/5/days during the intervention period. Susceptible depletion is assumed to be negligible. Solid black lines represent relative changes in the kernel: $F_t(\tau)/K_0(\tau)$. Solid vertical lines show the (fixed) mean intrinsic generation interval and dashed vertical lines the mean forward generation interval. See Supplementary Figure S1 for the impact of constant-strength and constant-speed interventions on instantaneous kernels.

165 between time t_{start} and t_{end} can be modeled as:

$$\mathcal{P}(t) = \begin{cases} 1 & t < t_{\text{start}} \\ \frac{1}{\theta} & t_{\text{start}} \leq t < t_{\text{end}} \\ 1 & t_{\text{end}} \leq t \end{cases} \quad (8)$$

Fig. 1A–C illustrates the impact of such intervention on the forward kernel $F_t(\tau)$ of an individual infected 5 days before t_{start} , 5 days after t_{start} , and 5 days before t_{end} . This constant-strength intervention reduces transmission immediately (Fig. 1A); likewise, lifting this intervention can, in theory, cause the forward kernel to return back to normal immediately (Fig. 1C). Even though the exact shape of the kernel $F_t(\tau)$ depends on the time of infection and when the intervention was introduced relative to the infection time, the relative impact of intervention in reducing transmission (black solid lines in Fig. 1A–C, representing $F_t(\tau)/K(0, \tau)$) is constant ($1/\theta$) for transmission that occurs during the intervention period.

Such intervention has predictable effects on forward generation intervals: implementing (lifting) intervention decreases (increases) future transmission potential and therefore decreases (increases) the mean forward generation interval (Fig. 1A,C). If an individual is infected after t_{start} (and much earlier than t_{end}), this intervention simply reduces the entire kernel by a constant amount and has no effect on realized generation intervals (Fig. 1B). This observation generalizes the phenomenon of contraction of realized generation intervals due to susceptible depletion (Kenah et al., 2008; Nishiura, 2010; Champredon and Dushoff, 2015).

On the other hand, the instantaneous kernel at time t corresponds to $K(t, \tau) = \mathcal{R}_0 \mathcal{P}(t) g_0(\tau)$, and changes in \mathcal{P} before or after time t (e.g., onset or offset of intervention) does not affect the shape of $K(t, \tau)$. Therefore, before the intervention is introduced, the instantaneous kernel is identical to the intrinsic kernel (Supplementary Figure S1A). During the intervention, the constant-strength intervention reduces the overall height of the kernel by a factor of θ but does not affect its shape otherwise (Supplementary Figure S1B–C). In other words, the onset and offset of constant-strength intervention does not affect the shape of the instantaneous generation-interval distribution—this property allowed previous studies to conclude that $\mathcal{R}_i(t)$ should be estimated with an intrinsic generation-interval distribution (Gostic et al., 2020).

Analogously, we consider a constant-speed intervention $\mathcal{I}(t, \tau) = \mathcal{H}(t, \tau)$ that depends on time-varying hazard of isolation $h(t)$:

$$\mathcal{H}(t, \tau) = \exp \left(- \int_0^\tau h(t - \sigma) d\sigma \right). \quad (9)$$

Analogous to the constant-strength intervention, the constant-speed intervention assumes a constant hazard of isolation across the age of infection τ at a given time t ; however, the hazard need not be constant across calendar time. Then, $\mathcal{H}(t, \tau)$ represents the probability that an individual infected τ time units ago has not been isolated by calendar time t . In practice, the hazard of isolation is expected to depend not only on calendar time t but also on the age of infection τ —for example, we expect $h(t, \tau)$ to increase with τ for symptom-based interventions to reflect the increasing cumulative probability of developing symptoms.

For example, a constant-speed intervention that takes place between time t_{start}

205 and t_{end} can be modeled using the following hazard function:

$$h(t) = \begin{cases} 0 & t < t_{\text{start}} \\ \phi & t_{\text{start}} \leq t < t_{\text{end}} \\ 0 & t_{\text{end}} \leq t \end{cases} \quad (10)$$

206 Since the forward kernel corresponds to $F_t(\tau) = \mathcal{R}_0 \mathcal{H}(t + \tau, \tau) g_0(\tau)$, the probabil-
 207 ity that an individual infected at time t has not been isolated by τ time units after
 208 infection depends on the amount of time the individual has been exposed to this
 209 intervention. If the individual is infected before t_{start} , they will not be isolated by this
 210 intervention until after t_{start} . If the individual is infected after t_{end} , they will never be
 211 isolated by this intervention. Fig. 1D–F illustrates the impact of such intervention
 212 on the forward kernel of an individual infected 5 days before t_{start} , at t_{start} , and 5 days
 213 before t_{end} . Unlike the constant-strength intervention, the constant-speed intervention
 214 does not show effects immediately; that is, the rate at which an infected individual
 215 generates secondary infections at time t_{start} remains unaffected by the intervention
 216 because it takes time to identify and isolate infected individuals. On the other hand,
 217 when the intervention is lifted at t_{end} , the value of the kernel at calendar time re-
 218 mains unchanged because some fraction of infected individuals have already been
 219 isolated. Constant-speed interventions always shorten realized generation intervals
 220 because they prevent late transmission (Fig. 1D–F).

221 The effect of constant-speed intervention on the instantaneous kernel, $K(t, \tau) =$
 222 $\mathcal{R}_0 \mathcal{H}(t, \tau) g_0(\tau)$, is less obvious. For individuals infected at time t , the forward kernel
 223 $F_t(\tau)$ depends on the hazard between time t and $t + \tau$ because $F_t(\tau)$ describes condi-
 224 tions *after* time t . On the other hand, the instantaneous kernel $K(t, \tau)$ depends on the
 225 hazard between time $t - \tau$ and t because $K(t, \tau)$ describes conditions *at* time t . Once
 226 again, before the constant-speed intervention is introduced, the instantaneous kernel
 227 is identical to the intrinsic kernel (Supplementary Figure S1D). During intervention,
 228 in particular when $t = t_{\text{start}} + x$, the instantaneous kernel reflects the first x days of
 229 constant-speed intervention effort: therefore, $K(t, \tau)/K(0, \tau)$ decreases for the first x
 230 days and plateaus (Supplementary Figure S1E–F). Constant-speed interventions also
 231 always shorten instantaneous generation intervals—we show later that the timing of
 232 reduction in forward and instantaneous generation intervals differs.

233 Finally, we can decompose the generalized intervention function $\mathcal{I}(t, \tau)$ as a prod-
 234 uct of constant-strength and constant-speed interventions: $\mathcal{I}(t, \tau) = \mathcal{P}(t) \mathcal{H}(t, \tau)$. In
 235 this case, the forward kernel corresponds to:

$$F_t(\tau) = \mathcal{R}_0 \mathcal{P}(t + \tau) \mathcal{H}(t + \tau, \tau) g_0(\tau), \quad (11)$$

236 which can be used to describe the dynamics of incidence $i(t)$ in the form of Eq. 5.
 237 Likewise, the instantaneous kernel corresponds to:

$$K(t, \tau) = \mathcal{R}_0 \mathcal{P}(t) \mathcal{H}(t, \tau) g_0(\tau), \quad (12)$$

which can be used to describe the dynamics of incidence $i(t)$ in the form of Eq. 3. In both case, the combined effects of constant-strength and constant-speed intervention can be understood in terms of the product of their marginal effects.

2.3 Quantifying changes in generation-interval distributions

In order to model the renewal process and accurately estimate $\mathcal{R}_i(t)$, we have to know how the instantaneous generation-interval distribution $g_t(\tau)$ changes across time t . The instantaneous distribution measures the infectiousness of an individual infected τ time units ago at time t and is therefore different from the distribution of realized generation intervals (i.e., time between actual infection events). For example, while both the forward generation-interval distribution $f_{t-\tau}(\tau)$ and the instantaneous generation-interval distribution $g_t(\tau)$ depend on the rate at which secondary cases at time t are generated by a primary case infected at time $t - \tau$, $K(t, \tau)$, they are normalized by different quantities:

$$f_{t-\tau}(\tau) = \frac{K(t, \tau)}{\int_0^\infty K(t - \tau + \sigma, \sigma) d\sigma} \neq \frac{K(t, \tau)}{\int_0^\infty K(t, \sigma) d\sigma} = g_t(\tau). \quad (13)$$

The forward distribution $f_{t-\tau}(\tau)$ is normalized by the average number of new infections caused by an individual infected at time $t - \tau$ (i.e., the case reproduction number, $\mathcal{R}_c(t - \tau)$). On the other hand, the instantaneous distribution $g_t(\tau)$ is normalized by a counterfactual measure of transmission $\mathcal{R}_i(t)$.

Rewriting Eq. 4 provides further insight into their differences:

$$f_t(\tau) = \frac{\mathcal{R}_i(t + \tau)g_{t+\tau}(\tau)}{\int \mathcal{R}_i(t + \sigma)g_{t+\sigma}(\sigma) d\sigma}. \quad (14)$$

Even if the instantaneous generation-interval distribution $g_t(\tau)$ remains invariant across calendar time t , changes in transmission conditions (and therefore $\mathcal{R}_i(t)$) can change the shape of the forward generation-interval distribution. For example, as we showed earlier, the forward generation-interval distribution changes under a constant-strength intervention even though the instantaneous generation-interval distribution does not. Therefore, renewal equation models that rely on the forward form (Eq. 5) with time-invariant $f_t(\tau)$ but changing \mathcal{R}_c should generally be avoided.

On the other hand, if we were to take all realized generation intervals that end at time t and form a distribution, we obtain what is known as the backward generation-interval distribution, $b_t(\tau)$:

$$b_t(\tau) = \frac{i_{t-\tau}(t)}{\int_0^\infty i_{t-\sigma}(t) d\sigma}. \quad (15)$$

The backward distribution systematically differs from the instantaneous distribution:

$$b_t(\tau) = \frac{g_t(\tau)i(t - \tau)}{\int_0^\infty g_t(\sigma)i(t - \sigma) d\sigma} \quad (16)$$

due to its dependence on previous incidence of infection. For example, when incidence is increasing exponentially, we are more likely to observe shorter generation intervals for a cohort of infectees that were infected at the same time because their infectors are more likely to have been infected recently.

Rewriting Eq. 16 in terms of the forward distribution shows that the backward distribution also depends on the case reproduction number $\mathcal{R}_c(t - \tau)$ of the cohort of infectors at time $t - \tau$:

$$b_t(\tau) = \frac{\mathcal{R}_c(t - \tau) f_{t-\tau}(\tau) i(t - \tau)}{\int_0^\infty \mathcal{R}_c(t - \sigma) f_{t-\sigma}(\sigma) i(t - \sigma) d\sigma}. \quad (17)$$

As defined in Eq. 15, the total density of generation intervals between time $t - \tau$ and time t corresponds to $i_{t-\tau}(t)$ (i.e., the total number of infections at time t caused by a cohort of individuals that were infected at time $t - \tau$), which depends on the incidence $i(t - \tau)$ at time $t - \tau$ as well as their average infectiousness $\mathcal{R}_c(t - \tau)$. In other words, a cohort of infectors that generated more infections will have greater contribution towards the backward generation-interval distribution at a given time. Several studies have noted, in various contexts, that backward distributions of epidemiological delays provide biased estimates of the forward distribution due to effects of this sort (Nishiura, 2010; Champredon and Dushoff, 2015; Park et al., 2020).

2.4 Quantifying changes in reproduction numbers

The instantaneous reproduction number $\mathcal{R}_i(t)$ provides a measure for the impact of intervention:

$$\mathcal{R}_i(t) = \int_0^\infty K(t, \sigma) d\sigma, \quad (18)$$

$$= \mathcal{R}_0 S(t) \mathcal{P}(t) \int_0^\infty \mathcal{H}(t, \sigma) g_0(\sigma) d\sigma. \quad (19)$$

Since $\mathcal{R}_i(t)$ measures conditions at time t , one would typically expect to detect changes in $\mathcal{R}_i(t)$ as soon as interventions are implemented—as we see in Eq. 19 (and also in Fig. 1), this is true for changes in a constant-strength intervention $\mathcal{P}(t)$ but not under a constant-speed intervention $\mathcal{H}(t, \sigma)$. Therefore, it has been previously argued that $\mathcal{R}_i(t)$ can provide a real-time measure for whether the disease will continue to spread or not (Gostic et al., 2020).

Estimating $\mathcal{R}_i(t)$ depends on the instantaneous generation-interval distribution $g_t(\tau)$, which can vary across time under constant-speed interventions:

$$g_t(\tau) = \frac{K(t, \tau)}{\mathcal{R}(t)} = \frac{\mathcal{H}(t, \tau) g_0(\tau)}{\int_0^\infty \mathcal{H}(t, \sigma) g_0(\sigma) d\sigma}. \quad (20)$$

By rearranging Eq. 2, we obtain the following estimator for $\mathcal{R}(t)$:

$$\mathcal{R}_i(t) = \frac{i(t)}{\int_0^\infty g_t(\sigma) i(t - \sigma) d\sigma}. \quad (21)$$

While this estimator is similar in form to previously proposed estimators (Fraser, 2007), it differs in allowing for the underlying instantaneous generation-interval distribution to vary across time. In particular, the popular R package **EpiEstim** uses this approach while assuming that the underlying instantaneous distribution does not change over time (Cori et al., 2013); such methods can accurately estimate changes in $\mathcal{R}_i(t)$ under constant-strength interventions, but not necessarily under more general conditions.

When both strength- and speed-like interventions are present during an ongoing epidemic, classical estimators (Fraser, 2007; Cori et al., 2013) measure a slightly different quantity:

$$\mathcal{R}_{g0}(t) = \frac{i(t)}{\int_0^\infty g_0(\sigma) i(t - \sigma) d\sigma}. \quad (22)$$

This is the number of infections per infection required to explain current incidence under the counter-factual that the generation-interval distribution has not changed. This estimator is widely used, because it is simple, often robust to estimate, and often a good proxy for \mathcal{R}_i . When interventions have speed-like components, however, the exact meaning of this estimator can be difficult to interpret; and it does not necessarily accurately reflect how conditions are changing through time.

The case reproduction number $\mathcal{R}_c(t)$ is similarly complicated. Since $\mathcal{R}_c(t)$ measures the average number of new infections caused by an individual infected at time t , we have

$$\mathcal{R}_c(t) = \frac{\int_0^\infty i_t(t + \sigma) d\sigma}{i(t)}, \quad (23)$$

where $i_t(t + \sigma)$ represents incidence at time $t + \sigma$ caused by individuals who were infected at time t . Substituting Eq. 15, it is straightforward to see that $\mathcal{R}_c(t)$ can be estimated by using the backward generation-interval distribution:

$$\mathcal{R}_c(t) = \frac{\int_0^\infty b_{t+\sigma}(\sigma) i(t + \sigma) d\sigma}{i(t)}. \quad (24)$$

Here, the numerator, which represents the total number of infections caused by individuals infected at time t , is calculated by multiplying future incidence $i(t + \sigma)$ with the probability that future infections are caused by an individual infected at time t $b_{t+\sigma}(\sigma)$. Using Eq. 16, we obtain a Wallinga-Teunis-like estimator (Wallinga and Teunis, 2004):

$$\mathcal{R}_c(t) = \int_0^\infty \left(\frac{g_{t+\sigma}(\sigma) i(t + \sigma)}{\int_0^\infty g_{t+\sigma}(\sigma') i(t + \sigma - \sigma') d\sigma'} \right) d\sigma. \quad (25)$$

This derivation clarifies that, like the classic estimator for \mathcal{R}_i , the classic estimator for \mathcal{R}_c is based on the intrinsic generation-interval distribution, and thus implicitly relies on the assumption that changes in transmission are strength-like and not speed-like.

Some studies have suggested substituting the forward distribution $f_t(\tau)$ instead to estimate the “time-varying” or the “effective” reproduction number $\mathcal{R}(t)$ (Liu et al., 2018; Ali et al., 2020):

$$\mathcal{R}_{\text{forward}}(t) = \frac{i(t)}{\int_0^\infty i(t-\sigma)f_{t-\sigma}(\sigma) d\sigma}. \quad (26)$$

This choice is potentially problematic, as the forward distribution differs systematically from the instantaneous distribution. For example, under constant-strength interventions, the forward distribution changes over time even though the instantaneous distribution remains time invariant—these differences can lead to systematic biases. In Section 3, we compare $\mathcal{R}_{\text{forward}}(t)$ with $\mathcal{R}_i(t)$ and $\mathcal{R}_c(t)$.

2.5 Quantifying changes in time-dependent growth rate

The instantaneous reproduction number $\mathcal{R}_i(t)$ provides a long-term threshold for whether the epidemic will *eventually* grow or decline if current conditions remain unchanged; perhaps counterintuitively, it does not tell us whether the epidemic is growing or not at a given moment. In contrast, the epidemic growth rate $r(t)$ does provide a convenient metric that is consistent with whether incidence is increasing or decreasing at a given time. Researchers often focus on the initial exponential growth rate, but we can look at the per-capita growth rate at any time:

$$r(t) = \frac{1}{i(t)} \frac{di(t)}{dt}. \quad (27)$$

By definition, incidence grows when $r(t) > 0$ (and vice versa)—thus, this provides an instantaneous threshold for incidence of infection (but does not provide information about the long-term behavior).

3 Example: Semi-mechanistic SIR model

In order to understand how constant-strength and constant-speed interventions affect disease spread, we use a semi-mechanistic SIR model to generate synthetic data and compare various estimates of $\mathcal{R}(t)$ and $r(t)$:

$$\frac{dS}{dt} = -\beta(t)SI, \quad (28)$$

$$\frac{dI}{dt} = \beta(t)SI - \gamma(t)I, \quad (29)$$

$$\frac{dR}{dt} = \gamma(t)I, \quad (30)$$

where S , I , R represent the proportion of individuals that are susceptible, infected, and removed (either due to recovery or isolation measures); $\beta(t)$ represents a time-varying transmission rate; and $\gamma(t)$ represents a time-varying removal rate. We refer

346 to this model as semi-mechanistic because the infection and recovery process are
 347 modeled explicitly, but changes in β and γ are allowed to change freely over time
 348 (without any mechanisms). In this case, the instantaneous kernel can be written as:

$$K(t, \tau) = \beta(t)S(t) \exp \left(- \int_{t-\tau}^t \gamma(s) ds \right). \quad (31)$$

349 Thus, changes that affect only the transmission rate $\beta(t)$ (respectively, removal rate
 350 $\gamma(t)$) exactly match the definition of constant-strength (constant-speed) interventions.
 351 Note also that an abrupt change in β will produce a parallel abrupt change in the ker-
 352 nel, and thus in incidence, while an abrupt change in $\gamma(t)$ will not have an immediate
 353 effect, due to delays in isolating individuals. Finally, the instantaneous reproduction
 354 number is given by:

$$\mathcal{R}_i(t) = \beta(t)S(t) \int_0^\infty \exp \left(- \int_{t-\tau}^t \gamma(s) ds \right) d\tau. \quad (32)$$

355 When $\gamma(t) \equiv \gamma(0)$, we obtain a familiar form: $\mathcal{R}_i(t) = \mathcal{R}_0 S(t)$, where $\mathcal{R}_0 =$
 356 $\beta(0)/\gamma(0)$. Note, however, that in the general case the “instantaneous” \mathcal{R}_i depends on
 357 past values of γ : the “conditions” that are held constant refer not to the current value
 358 of γ but to the current distribution of the kernel across τ . *[JD: In some cases it will*
 359 *be of interest to define yet another (even-more-instantaneous) reproductive number.*
 360 *Might be hard to squeeze into this framework, but might be worth discussing.]*

361 Here, we compare two different scenarios, in which interventions are introduced
 362 and are later partially lifted (Fig. 2): one a smooth introduction and lifting of a
 363 constant-strength intervention, modeled by changing in β while fixing γ (Fig. 2A);
 364 the other a sudden introduction and lifting of a constant-speed intervention, modeled
 365 by changing in γ while fixing β (Fig. 2B). We construct these two to give identical
 366 incidence curves (Fig. 2C), and thus refer to them as *equivalent* interventions. This
 367 equivalence shows that changes in β and γ cannot in general be jointly identified
 368 from the incidence curve alone (see Methods and Materials). In both cases, growth
 369 rate $r(t)$ estimates are identical (Fig. 2D); as we show later, however, reproduction
 370 numbers differ between the two scenarios.

371 Epidemiological dynamics under a constant-strength intervention are presented
 372 in Fig. 3. In this case, the proportional reproduction number $\mathcal{R}_{g0}(t)$, which relies
 373 on the intrinsic generation-interval distribution, matches the instantaneous reproduc-
 374 tion number $\mathcal{R}_i(t)$, which relies on the instantaneous generation-interval distribution
 375 (Fig. 3A). Therefore, we are able to correctly estimate $\mathcal{R}_i(t)$ using **EpiEstim** (Fig. 3A).
 376 The initial overestimation from **EpiEstim** is caused by the left censoring (Gostic et al.,
 377 2020). Minor differences between **EpiEstim** estimates and $\mathcal{R}_{g0}(t)$ are caused by dis-
 378 cretization.

379 Likewise, we can accurately estimate the case reproduction number $\mathcal{R}_c(t)$ using
 380 the classic Wallinga-Teunis estimator (based on the intrinsic generation-interval distri-
 381 bution) (Fig. 3B). This is because the instantaneous generation-interval distribution

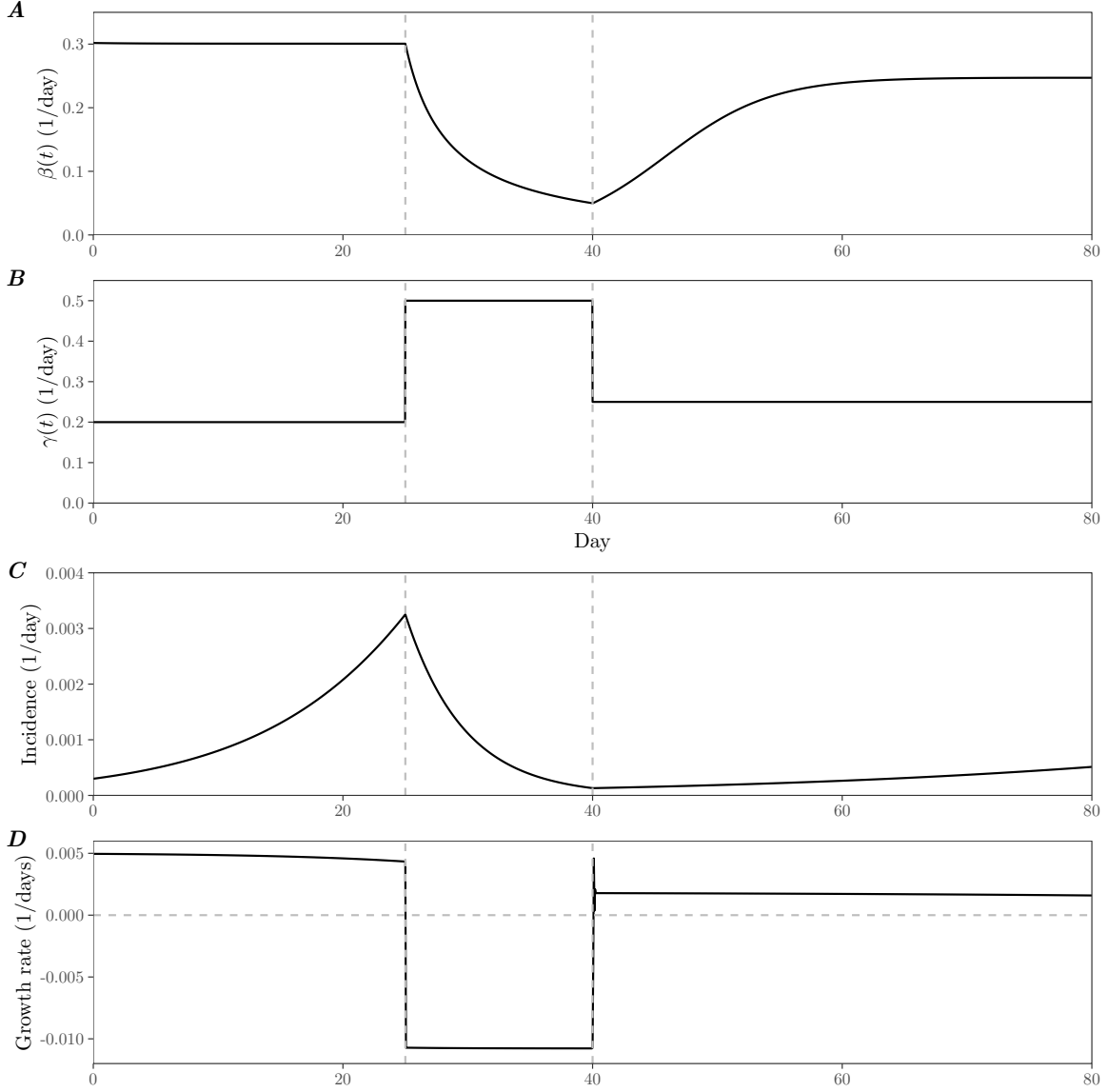


Figure 2: Assumed changes in transmission and removal rate. The semi-mechanistic SIR model is simulated under two different scenarios. (A) Equivalent constant-strength intervention scenario. Removal rate γ is fixed to 0.2/day throughout. (B) Equivalent constant-speed intervention scenario. Transmission rate β is fixed to 0.3/day throughout. (C) Instantaneous incidence under equivalent constant-strength and constant-speed intervention scenarios (both scenarios give identical incidence trajectories). (D) Growth rate estimates over time.

382 does not change over time under constant-strength interventions (Fig. 3C). Using
 383 the forward generation-interval distribution, instead of the instantaneous generation-
 384 interval distribution, matches neither $\mathcal{R}_i(t)$ ($\mathcal{R}_{\text{forward}}(t)$ in Fig. 3A) nor $\mathcal{R}_c(t)$ in this
 385 case ($\mathcal{R}_{\text{forward}}(t)$ in Fig. 3B) because the forward distribution changes, even when the

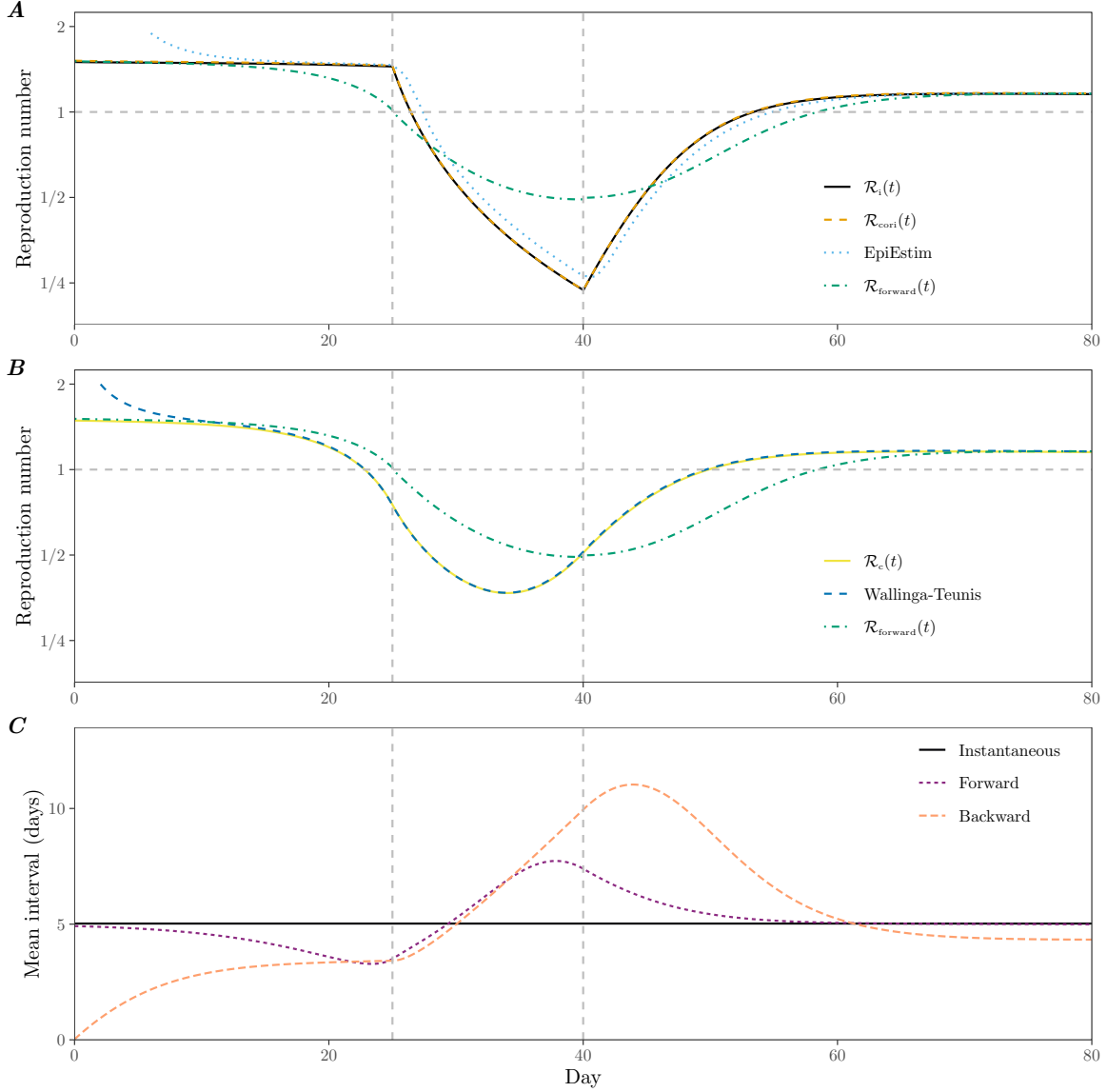


Figure 3: Epidemiological dynamics of a semi-mechanistic SIR model under equivalent constant-strength intervention. (A) Changes in true instantaneous reproduction number $\mathcal{R}_i(t)$, proportional reproduction number $\mathcal{R}_{g0}(t)$, estimated $\mathcal{R}_i(t)$ using EpiEstim (assuming a population of one million), and estimated $\mathcal{R}_{forward}(t)$ using the forward generation-interval distribution. (B) Changes in true case reproduction number $\mathcal{R}_c(t)$, estimated $\mathcal{R}_c(t)$ using Wallinga-Teunis estimator with intrinsic generation-interval distribution, and estimated $\mathcal{R}_{forward}(t)$ using the forward generation-interval distribution. (C) Changes in mean instantaneous, forward, and backward generation intervals.

instantaneous distribution does not change (Fig. 3C). As described earlier (Fig. 1A–C), introducing and lifting a constant-strength intervention cause the forward gen-

eration intervals become shorter and longer, respectively (Fig. 3C). The backward distribution exaggerates these changes through the epidemic growth/decay effect—when an epidemic is growing (decaying), the mean backward intervals become shorter (longer).

Epidemiological dynamics under a constant-speed intervention are presented in Fig. 4. In this case, the instantaneous generation-interval distribution changes through time. $\mathcal{R}_{g0}(t)$ differs from the true $\mathcal{R}_i(t)$ (Fig. 4A) because the constant-speed interventions lead to changes in the instantaneous generation-interval distribution (Fig. 4C). Therefore, EpiEstim inaccurately estimates $\mathcal{R}_i(t)$ (Fig. 4A)—in particular, EpiEstim estimates that $\mathcal{R}_i(t)$ crossed the threshold $\mathcal{R}_i(t) = 1$ later (around $t = 55$) than it actually did (around $t = 45$).

Using the intrinsic distribution is also problematic for estimating the case reproduction number $\mathcal{R}_c(t)$ (Fig. 4B). The true $\mathcal{R}_c(t)$ changes sharply, reflecting sharp changes in the removal rate $\gamma(t)$ (Fig. 2B), but using the intrinsic distribution gives smooth estimates of $\mathcal{R}_c(t)$. In this case, $\mathcal{R}_{\text{forward}}(t)$ matches $\mathcal{R}_i(t)$ and $\mathcal{R}_c(t)$ better than their corresponding estimates using the intrinsic generation-interval distribution (EpiEstim and Wallinga-Teunis in Fig. 4, respectively) because the forward generation-interval distribution captures the effects of the constant-speed intervention (Fig. 4C). Surprisingly, the backward generation-interval distribution stays nearly constant because the effect of decreasing incidence (which lengthens the backward generation intervals) cancels out with that of shorter realized generation intervals, caused by the constant-speed intervention (Fig. 4C).

Comparing simulations under equivalent constant-strength and constant-speed interventions allows us to better understand the differences between the $\mathcal{R}_i(t)$ and $r(t)$ in capturing current conditions at time t . Under a constant-strength intervention, $\mathcal{R}_i(t) = \beta(t)/\gamma(0)$, and therefore $\mathcal{R}_i(t)$ crosses the threshold, $\mathcal{R}_i(t) = 1$, when $\beta(t)$ crosses the threshold, $\beta(t) = \gamma(0)$ (compare Fig. 2A with Fig. 3A). Under a constant-speed intervention, however, sharp changes in $\gamma(t)$ translate to smooth changes in $\mathcal{R}_i(t)$, and therefore $\mathcal{R}_i(t)$ crosses the threshold, $\mathcal{R}_i(t) = 1$, later (compare Fig. 2B with Fig. 4A). Instead, sharp changes in $\gamma(t)$ are captured by sharp changes in $r(t)$ (compare Fig. 2B with Fig. 2D)—this can readily be seen by calculating $r(t)$ as the logarithmic derivative of the instantaneous incidence $i(t) = \beta(t)SI$.

$$r(t) = \frac{1}{i(t)} \frac{di(t)}{dt} = \frac{1}{\beta(t)} \frac{d\beta(t)}{dt} - \beta(t)I + \beta(t)S - \gamma(t). \quad (33)$$

Eq. 33 also reinforces that the effect of changes in $\beta(t)$ on $r(t)$ are not straightforward, but are affected by per-capita changes in both S and I . Therefore, $\mathcal{R}_i(t)$ is a better measure for capturing current conditions at time t under constant-strength interventions, whereas $r(t)$ is better for capturing current conditions at time t under constant-speed interventions.

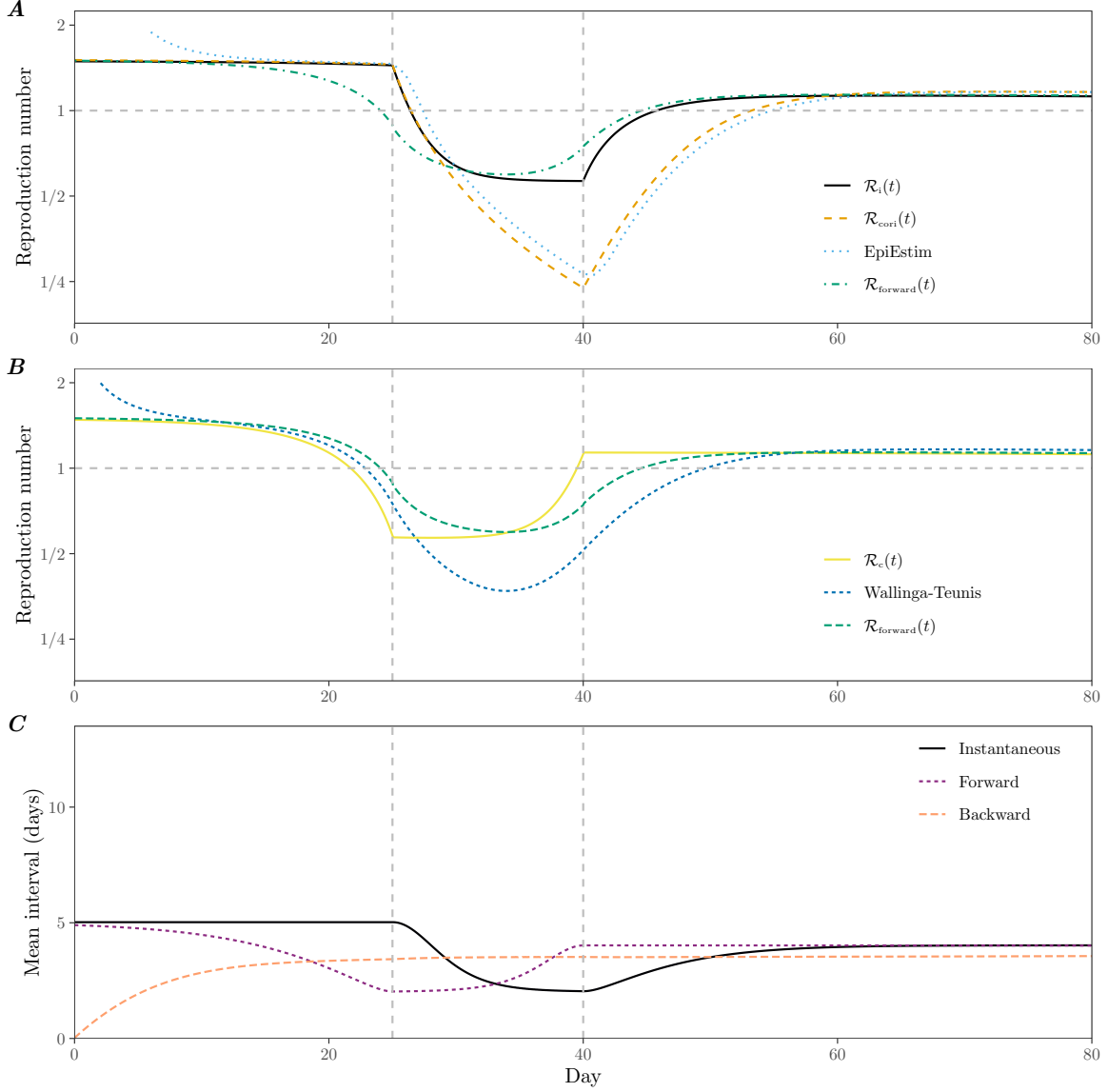


Figure 4: **Epidemiological dynamics of a semi-mechanistic SIR model under equivalent constant-speed intervention.** (A) Changes in true instantaneous reproduction number $\mathcal{R}_i(t)$, proportional reproduction number $\mathcal{R}_{g0}(t)$, estimated $\mathcal{R}_i(t)$ using EpiEstim (assuming a population of one million), and estimated $\mathcal{R}_{forward}(t)$ using the forward generation-interval distribution. (B) Changes in true case reproduction number $\mathcal{R}_c(t)$, estimated $\mathcal{R}_c(t)$ using Wallinga-Teunis estimator with intrinsic generation-interval distribution, and estimated $\mathcal{R}_{forward}(t)$ using the forward generation-interval distribution. (C) Changes in mean instantaneous, forward, and backward generation intervals.

4 Discussion

The impact of epidemic interventions are often characterized by changes in “effective” reproduction numbers, $\mathcal{R}(t)$. Many statistical softwares have been developed to accurately estimate $\mathcal{R}(t)$, but the majority of existing frameworks neglect possibility that the underlying generation-interval distribution can change over time—an insight that goes back > 10 years (Fraser, 2007). Here, we distinguish two reproduction numbers—instantaneous reproduction number $\mathcal{R}_i(t)$ and case reproduction number $\mathcal{R}_c(t)$, which describe counterfactual and realized transmission processes, respectively—and show that both reproduction numbers can correctly describe the renewal process of infection when paired with correct generation-interval distributions. In particular, a counterfactual distribution, which we call the instantaneous generation-interval distribution, is required to correctly estimate the instantaneous reproduction number. This distribution is affected by constant-speed, but not constant-strength, interventions. Neglecting changes in this distribution gives biased estimates of $\mathcal{R}_i(t)$, including estimates of when $\mathcal{R}_i(t)$ crosses the threshold value of 1. Instead, time-dependent growth rate $r(t)$ is a better measure for characterizing the impact of epidemic intervention under a constant-speed intervention.

In practice, estimating the instantaneous generation-interval distribution is expected to be difficult as it systematically differs from the realized generation intervals: even if we can observe all realized generation intervals throughout an epidemic, estimating the instantaneous distribution $g(t, \tau)$ is not trivial. For example, even within a homogeneously mixing population, in which the disease is allowed to spread unchecked (and therefore $g(t, \tau) = g_0(\tau)$ for all t), aggregating all realized generation intervals underestimates the mean intrinsic generation interval due to susceptible depletion (Park et al., 2020). Novel statistical methods are needed to accurately estimate the instantaneous distribution $g(t, \tau)$.

Most state-of-art statistical softwares for estimating reproduction numbers assume that the instantaneous generation-interval distribution does not change across time (e.g., (Abbott et al., 2020; Flaxman et al., 2020; Brauner et al., 2021)). We refer to these estimates as proportional reproduction numbers (\mathcal{R}_{g0} above) as they capture proportional reduction in incidence, rather than transmission. While this approach is parsimonious, practical and useful, it is important that researchers recognize the dependence on this assumption. This reproduction number estimate can differ systematically from the true instantaneous reproduction number \mathcal{R}_i under speed-like interventions such as contact tracing. Emergence of variants with a different infectiousness profile (and therefore the intrinsic generation-interval distribution) can have similar effects.

In the context of the current SARS-CoV-2 pandemic, assuming a time-invariant generation-interval distribution was justifiable during the early period when most interventions were strength-like, including lockdowns, school closures, and travel bans (Flaxman et al., 2020; Li et al., 2021; Brauner et al., 2021). Nonetheless, speed-like interventions, including intense contact-tracing efforts (Park et al., 2020) and

introduction of contact tracing apps (Wymant et al., 2021), had clear, non-negligible impact on the overall spread; these interventions, including awareness-driven behavioral changes (which can cause symptomatic individuals to self-isolate faster), are likely to have shortened the instantaneous generation intervals by preventing transmission during later stages of infection. Therefore, current estimates of \mathcal{R}_i that rely on early estimates of the generation-interval distributions should be reassessed. Future studies should also consider incorporating hazard-based changes for modeling speed-like interventions.

The renewal-equation framework based on the instantaneous form (Eq. 3) has been widely used in epidemic modeling due to its flexibility. A few studies relied on the forward form (Eq. 5), but they assumed a time-invariant generation-interval distribution (Nishiura, 2007; Alvarez et al., 2020; White et al., 2021). As discussed above, the forward generation-interval distribution, which correctly links the case reproduction number with case counts, is expected to change over time. To our knowledge, this is the first study to formally link the case reproduction number with the forward renewal equation and to demonstrate the equivalence between the forward and instantaneous renewal formulations.

This study highlights the complementary nature of time-varying reproduction number $\mathcal{R}(t)$ and growth rate $r(t)$ as measures for describing epidemic dynamics (Dushoff and Park, 2021). In particular, $r(t)$ can always be reliably estimated (given high-quality incidence data) but does not accurately reflect changes in current conditions, except when changes are predominantly speed-like. Conversely, $\mathcal{R}(t)$ – and particularly the instantaneous reproductive number $\mathcal{R}_i(t)$ – provides an accurate reflection of current conditions in *theory*, but can only be reliably estimated from incidence data alone when changes are primarily strength-like. Methods that use real-time information about *changes* in disease-transmission intervals have the potential to unify these frameworks, but will often be limited by the difficulty of collecting sufficient high-quality data.

5 Methods

5.1 Equivalent constant-strength and constant-speed interventions

We model a simple scenario in which a flu-like pathogen with $\mathcal{R}_0 = 1.5$ invades an immunologically naive population using the semi-mechanistic SIR model (Eq. 28–Eq. 30). We begin by modeling constant-speed intervention and find the equivalent constant-strength intervention. In particular, we assume that the disease spreads without any intervention in the beginning; on day 25, an intense case isolation measure is implemented; and on day 40, the intervention is partially lifted. This is modeled

504 as follows:

$$\beta(t) = 0.3 \text{ days}^{-1}, \gamma(t) = \begin{cases} 0.2 \text{ days}^{-1} & t < 25 \\ 0.5 \text{ days}^{-1} & 25 \leq t < 40 \\ 0.25 \text{ days}^{-1} & 40 \leq t \end{cases} \quad (34)$$

505 Simulations are run for 100 days based on the following initial conditions: $S(0) =$
 506 $1 - 10^{-3}$, $I(0) = 10^{-3}$, and $R(0) = 0$.

507 Since we assume that incidence is known exactly until time t^* we can estimate
 508 the transmission rate $\beta^*(t)$ (with fixed $\gamma(t) = \gamma(0)$) that gives an identical incidence
 509 trajectory until time $t < t^*$. This transmission rate is given by:

$$\beta^*(t) = \frac{\mathcal{R}_{g0}(t)\gamma(0)}{S(t)}, \quad (35)$$

510 where the proportional reproduction number \mathcal{R}_{g0} is calculated from the incidence
 511 curve $i(t)$ for time $t < t^*$. More generally, given true incidence $i(t)$ until time t^* ,
 512 modulated by any interventions, we can find equivalent constant-strength intervention
 513 $\mathcal{P}^*(t)$ until time t^* :

$$\mathcal{P}^*(t) = \frac{\mathcal{R}_{g0}(t)}{\mathcal{R}_0 S(t)}, \quad (36)$$

514 which generates an identical incidence curve when the initial conditions are identical.

Supplementary Materials

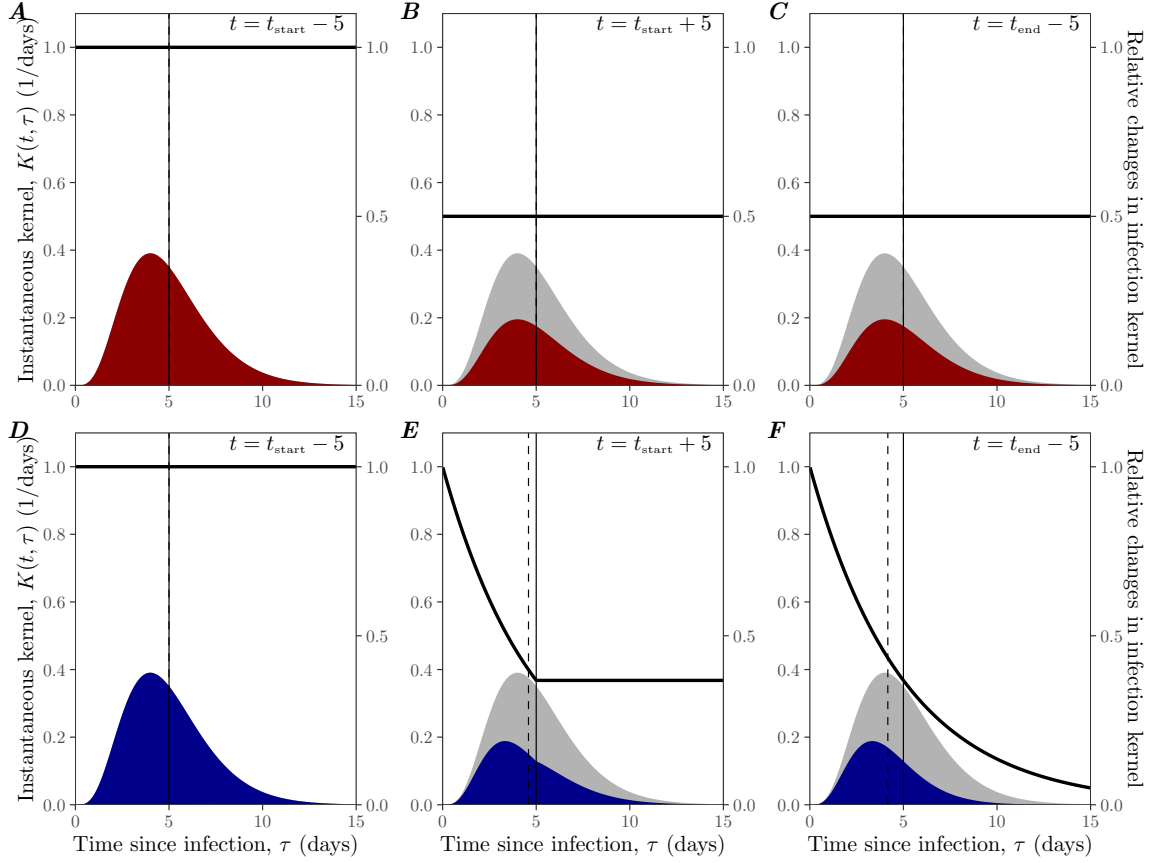


Figure S1: The impact of constant-strength and constant-speed interventions on instantaneous kernels. The impact of constant-strength (A–C) and constant-speed (D–F) intervention on instantaneous kernels at different time: 5 days before intervention onset (A, D), during intervention (B, E), and 5 days before intervention offset (C, F). Gray shaded curves represent the (fixed) intrinsic kernel $K_0(\tau)$, which is modeled using a gamma distribution with \mathcal{R}_0 of 2, a mean of 5 days and a squared coefficient of variation of 0.2. Colored curves represent the instantaneous kernel $K(t, \tau)$ under constant-strength (A–C) and constant-speed (D–F) interventions. The constant-strength intervention is assumed to reduce kernel by a factor of 2. The constant-speed intervention is assumed to have a constant hazard of 1/5/days during the intervention period. Susceptible depletion is assumed to be negligible. Solid black lines represent relative changes in the kernel: $K(t, \tau)/K_0(\tau)$. Solid vertical lines show the (fixed) mean intrinsic generation interval and dashed vertical lines the mean instantaneous generation interval.

References

- Abbott, S., J. Hellewell, R. Thompson, K. Sherratt, H. Gibbs, N. Bosse, J. Munday, S. Meakin, E. Doughty, J. Chun, Y. Chan, F. Finger, P. Campbell, A. Endo, C. Pearson, A. Gimma, T. Russell, n. null, S. Flasche, A. Kucharski, R. Eggo, and S. Funk (2020). Estimating the time-varying reproduction number of SARS-CoV-2 using national and subnational case counts [version 2; peer review: 1 approved with reservations]. *Wellcome Open Research* 5(112).
- Aldis, G. and M. Roberts (2005). An integral equation model for the control of a smallpox outbreak. *Mathematical biosciences* 195(1), 1–22.
- Ali, S. T., L. Wang, E. H. Lau, X.-K. Xu, Z. Du, Y. Wu, G. M. Leung, and B. J. Cowling (2020). Serial interval of SARS-CoV-2 was shortened over time by non-pharmaceutical interventions. *Science* 369(6507), 1106–1109.
- Alvarez, L., M. Colom, and J.-M. Morel (2020). A variational model for computing the effective reproduction number of sars-cov-2. *medRxiv*.
- Anderson, R. M. and R. M. May (1991). *Infectious diseases of humans: dynamics and control*. Oxford university press.
- Brauner, J. M., S. Mindermann, M. Sharma, D. Johnston, J. Salvatier, T. Gavenčiak, A. B. Stephenson, G. Leech, G. Altman, V. Mikulik, et al. (2021). Inferring the effectiveness of government interventions against COVID-19. *Science* 371(6531).
- Champredon, D. and J. Dushoff (2015). Intrinsic and realized generation intervals in infectious-disease transmission. *Proceedings of the Royal Society B: Biological Sciences* 282(1821), 20152026.
- Champredon, D., J. Dushoff, and D. J. D. Earn (2018). Equivalence of the Erlang-distributed SEIR epidemic model and the renewal equation. *SIAM Journal on Applied Mathematics* 78(6), 3258–3278.
- Cori, A., N. M. Ferguson, C. Fraser, and S. Cauchemez (2013). A new framework and software to estimate time-varying reproduction numbers during epidemics. *American journal of epidemiology* 178(9), 1505–1512.
- Diekmann, O. and J. A. P. Heesterbeek (2000). *Mathematical epidemiology of infectious diseases: model building, analysis and interpretation*, Volume 5. John Wiley & Sons.
- Diekmann, O., J. A. P. Heesterbeek, and J. A. Metz (1990). On the definition and the computation of the basic reproduction ratio \mathcal{R}_0 in models for infectious diseases in heterogeneous populations. *Journal of mathematical biology* 28(4), 365–382.

550 Dushoff, J. and S. W. Park (2021). Speed and strength of an epidemic intervention.
551 *Proceedings of the Royal Society B* 288(1947), 20201556.

552 Flaxman, S., S. Mishra, A. Gandy, H. J. T. Unwin, T. A. Mellan, H. Coupland,
553 C. Whittaker, H. Zhu, T. Berah, J. W. Eaton, et al. (2020). Estimating the effects
554 of non-pharmaceutical interventions on COVID-19 in europe. *Nature* 584(7820),
555 257–261.

556 Fraser, C. (2007). Estimating individual and household reproduction numbers in an
557 emerging epidemic. *PloS one* 2(8), e758.

558 Gostic, K. M., L. McGough, E. B. Baskerville, S. Abbott, K. Joshi, C. Tedijanto,
559 R. Kahn, R. Niehus, J. A. Hay, P. M. De Salazar, et al. (2020). Practical consid-
560 erations for measuring the effective reproductive number, R_t . *PLoS computational*
561 *biology* 16(12), e1008409.

562 Heesterbeek, J. and K. Dietz (1996). The concept of \mathcal{R}_0 in epidemic theory. *Statistica*
563 *Neerlandica* 50(1), 89–110.

564 Kenah, E., M. Lipsitch, and J. M. Robins (2008). Generation interval contraction
565 and epidemic data analysis. *Mathematical biosciences* 213(1), 71–79.

566 Li, Y., H. Campbell, D. Kulkarni, A. Harpur, M. Nundy, X. Wang, H. Nair, U. N.
567 for COVID, et al. (2021). The temporal association of introducing and lifting
568 non-pharmaceutical interventions with the time-varying reproduction number (R)
569 of SARS-CoV-2: a modelling study across 131 countries. *The Lancet Infectious*
570 *Diseases* 21(2), 193–202.

571 Liu, Q.-H., M. Ajelli, A. Aleta, S. Merler, Y. Moreno, and A. Vespignani (2018). Mea-
572 surability of the epidemic reproduction number in data-driven contact networks.
573 *Proceedings of the National Academy of Sciences* 115(50), 12680–12685.

574 Nishiura, H. (2007). Time variations in the transmissibility of pandemic influenza in
575 Prussia, Germany, from 1918–19. *Theoretical Biology and Medical Modelling* 4(1),
576 1–9.

577 Nishiura, H. (2010). Time variations in the generation time of an infectious dis-
578 ease: implications for sampling to appropriately quantify transmission potential.
579 *Mathematical Biosciences & Engineering* 7(4), 851.

580 Pan, A., L. Liu, C. Wang, H. Guo, X. Hao, Q. Wang, J. Huang, N. He, H. Yu, X. Lin,
581 et al. (2020). Association of public health interventions with the epidemiology of
582 the COVID-19 outbreak in Wuhan, China. *Jama* 323(19), 1915–1923.

583 Parag, K. V., R. N. Thompson, and C. A. Donnelly. Are epidemic growth rates more
584 informative than reproduction numbers? *Journal of the Royal Statistical Society:*
585 *Series A (Statistics in Society)* n/a(n/a).

- 586 Park, S. W., D. Champredon, and J. Dushoff (2020). Inferring generation-interval
587 distributions from contact-tracing data. *Journal of the Royal Society Inter-*
588 *face* 17(167), 20190719.
- 589 Park, S. W., K. Sun, D. Champredon, M. Li, B. M. Bolker, D. J. Earn, J. S. Weitz,
590 B. T. Grenfell, and J. Dushoff (2020). Forward-looking serial intervals correctly link
591 epidemic growth to reproduction numbers. *Proceedings of the National Academy*
592 *of Sciences* 118(2).
- 593 Park, Y. J., Y. J. Choe, O. Park, S. Y. Park, Y.-M. Kim, J. Kim, S. Kweon, Y. Woo,
594 J. Gwack, S. S. Kim, et al. (2020). Contact tracing during coronavirus disease
595 outbreak, South Korea, 2020. *Emerging infectious diseases* 26(10), 2465–2468.
- 596 Roberts, M. (2004). Modelling strategies for minimizing the impact of an imported
597 exotic infection. *Proceedings of the Royal Society of London. Series B: Biological*
598 *Sciences* 271(1555), 2411–2415.
- 599 Roberts, M. and J. Heesterbeek (2007). Model-consistent estimation of the basic re-
600 production number from the incidence of an emerging infection. *Journal of math-*
601 *ematical biology* 55(5-6), 803.
- 602 Svensson, Å. (2007). A note on generation times in epidemic models. *Mathematical*
603 *biosciences* 208(1), 300–311.
- 604 Wallinga, J. and P. Teunis (2004). Different epidemic curves for severe acute respi-
605 ratory syndrome reveal similar impacts of control measures. *American Journal of*
606 *epidemiology* 160(6), 509–516.
- 607 White, L. F., C. B. Moser, R. N. Thompson, and M. Pagano (2021). Statistical esti-
608 mation of the reproductive number from case notification data. *American Journal*
609 *of Epidemiology* 190(4), 611–620.
- 610 Wymant, C., L. Ferretti, D. Tsallis, M. Charalambides, L. Abeler-Dörner, D. Bonsall,
611 R. Hinch, M. Kendall, L. Milsom, M. Ayres, C. Holmes, M. Briers, and C. Fraser
612 (2021). The epidemiological impact of the NHS COVID-19 App. *Nature*.